Enhancing the thermoelectric figure of merit through the reduction of bipolar thermal conductivity with heterostructure barriers

Je-Hyeong Bahk and Ali Shakouri

Articles you may be interested in

Publisher's Note: "Dramatic thermal conductivity reduction by nanostructures for large increase in thermoelectric figure-of-merit of FeSb2" [Appl. Phys. Lett. 99, 163101 (2011)]
Appl. Phys. Lett. **100**, 059902 (2012); 10.1063/1.3679439

Enhanced thermoelectric figure of merit in SiGe alloy nanowires by boundary and hole-phonon scattering
J. Appl. Phys. **110**, 074317 (2011); 10.1063/1.3647575

High thermoelectric figure of merit in the Cu3SbSe4-Cu3SbS4 solid solution
Appl. Phys. Lett. **98**, 261911 (2011); 10.1063/1.3605246

Enhanced thermoelectric figure of merit in nanocrystalline Bi 2 Te 3 bulk
J. Appl. Phys. **105**, 094303 (2009); 10.1063/1.3120865

Enhanced thermoelectric figure of merit in nanostructured n -type silicon germanium bulk alloy
Appl. Phys. Lett. **93**, 193121 (2008); 10.1063/1.3027060

Enhancing the thermoelectric figure of merit through the reduction of bipolar thermal conductivity with heterostructure barriers

Je-Hyeong Bahk[a)] and Ali Shakouri

Birck Nanotechnology Center, Purdue University, West Lafayette, Indiana 47907, USA

In this paper, we present theoretically that the thermoelectric figure of merit for a semiconductor material with a small band gap can be significantly enhanced near the intrinsic doping regime at high temperatures via the suppression of bipolar thermal conductivity when the minority carriers are selectively blocked by heterostructure barriers. This scheme is particularly effective in nanostructured materials where the lattice thermal conductivity is lowered by increased phonon scatterings at the boundaries, so that the electronic thermal conductivity including the bipolar term is limiting the figure of merit zT. We show that zT can be enhanced to above 3 for p-type PbTe, and above 2 for n-type PbTe at 900 K with minority carrier blocking, when the lattice thermal conductivity is as low as 0.3 W/m K. © 2014 AIP Publishing LLC. [http://dx.doi.org/10.1063/1.4892653]

Thermoelectric energy conversion is a viable solid-state technology that can be used for improving fuel economy of heat engines via low temperature waste heat recovery or high temperature topping cycle applications.[1,2] The energy conversion efficiency of a thermoelectric device is directly related to the material's dimensionless thermoelectric figure of merit, $zT = S^2\sigma T/\kappa$, where S is Seebeck coefficient, σ is electrical conductivity, T is absolute temperature, and κ is total thermal conductivity. In the numerator, $S^2\sigma$ is called the power factor and is determined by electron and/or hole transport in the material. The total thermal conductivity in the denominator is the sum of the lattice and electronic contributions given by $\kappa = \kappa_l + \kappa_e$. The electronic thermal conductivity comprises the unipolar electronic thermal conductivities of electrons and holes and the bipolar thermal conductivity such that $\kappa_e = \kappa_{\rm elec} + \kappa_{\rm hole} + \kappa_{\rm bi}$.

Conventional thermal conductivity measurement techniques[3–5] cannot separate the electronic and lattice thermal conductivities. For single carrier transport, the electronic thermal conductivity is calculated by the Wiedemann-Franz relation[6] and then subtracted from the measured total thermal conductivity to obtain the lattice thermal conductivity. The Lorenz number used in the Wiedemann-Franz relation needs to be adjusted from the conventional value (2.45×10^{-8} W Ω K^{-2}), which is only valid in the degenerate limit or in metals, using careful electron transport modeling, since the Lorenz number is a function of band structure and Fermi level position.[7,8]

In the case of bipolar transport, a common method to separate bipolar thermal conductivity from lattice thermal conductivity is to perform a linear fitting of the total thermal conductivity after the unipolar electronic terms are subtracted, i.e., $(\kappa_l + \kappa_{\rm bi})$ vs. $1/T$ at the intermediate temperature regime where the bipolar term is negligible and the lattice thermal conductivity has $1/T$ dependence due to Umklapp processes. One can then identify the difference between the $(\kappa_l + \kappa_{bi})$ curve and the extrapolated linear fitting line at high temperatures to obtain the bipolar thermal conductivity.[9] This method, however, can lead to a large error since even a slight variation in the slope of the fitting line at the

intermediate temperature region can result in a large uncertainty in the extracted bipolar thermal conductivity value at high temperatures. Also lattice thermal conductivity does not always follow $\sim 1/T$ since the phonon scattering is typically a combination of several different scattering mechanisms that have different temperature dependencies. Instead, both bipolar and unipolar electronic thermal conductivities can be accurately calculated using the Boltzmann transport equations with band structure information for both the conduction and valence bands.[10] Also noted is that at high temperatures where bipolar thermal conductivity has a significant contribution, it is important to minimize radiation losses or other factors that can impact thermal conductivity measurements.

In the past decade, a significant reduction of lattice thermal conductivity due to increased phonon scattering via alloying and nanostructuring has been reported in various nanostructured bulk materials.[11–13] A very high $zT \sim 2.2$ was recently reported for bulk spark-plasma-sintered Na-doped PbTe:SrTe at 900 K, which the authors attributed to a significant reduction in the lattice thermal conductivity by the all-scale hierarchical material structures ranging from a few nano-meters to micro-meters in size.[14] Other nanostructured PbTe-based alloys, such as PbTe$_{1-x}$Se$_x$, PbTe:Ag$_2$Te, and PbTe:MTe (M = Cd, Hg), also showed reduced lattice thermal conductivity of 0.5–1.0 W/m K to achieve an enhanced zT of 1.4–1.8 at 700–800 K.[15–18] The n-type Mg$_2$Sn$_x$Si$_{1-x}$ alloys showed $zT \sim 1.3$ for $x = 0.6 \sim 0.7$ at 700 K due to the enhanced power factor by band convergence and the reduced lattice thermal conductivity by alloying and inherent nano-structuring.[19] In these papers, however, the bipolar thermal conductivity was not fully separated from the lattice thermal conductivity, so the lattice thermal conductivity values may be overestimated. In fact, accurate electron transport modeling based on the Boltzmann transport equation for the 2% Na-doped PbTe samples in Ref. 8 showed that the bipolar thermal conductivity was as large as 0.16 W/m K at 780 K, which is more than 30% of the lattice thermal conductivity ($\sim$0.5 W/m K). Also, the experimental thermal conductivity data for Mg$_2$Sn$_x$Si$_{1-x}$ alloys from Ref. 19 were later analyzed with a multiparabolic-band Boltzmann transport model to find a bipolar thermal conductivity as high as 1.0 W/m K

---

a)Electronic mail: jbahk@purdue.edu

at 800 K for the high Sn content sample ($x = 0.8$) even at a very high doping density $\sim 2 \times 10^{20}\,\mathrm{cm}^{-3}$ due to its small band gap.[20] It is essential, therefore, to apply careful electron transport modeling in order to accurately extract lattice and bipolar thermal conductivities.

Bipolar thermal conductivity originates from the bipolar thermodiffusion process in the material and is given by[21]

$$\kappa_{\mathrm{bi}} = \frac{\sigma_{\mathrm{elec}}\sigma_{\mathrm{hole}}}{\sigma_{\mathrm{elec}} + \sigma_{\mathrm{hole}}}(S_{\mathrm{elec}} - S_{\mathrm{hole}})^2 T, \quad (1)$$

where the subscripts, "elec" and "hole," denote the partial properties of electrons and holes, respectively. These partial properties can be calculated by separating the transport components occurring in the conduction band and the valence band using, for example, Boltzmann transport calculations. Equation (1) is approximately given near the intrinsic regime by

$$\kappa_{\mathrm{bi}} \propto \exp\left(-\frac{E_g}{2k_B T}\right), \quad (2)$$

where E_g is the band gap, and k_B is the Boltzmann constant. According to Eq. (2), the bipolar thermal conductivity increases exponentially with increasing temperature at a given doping density, and the smaller the band gap, the larger the bipolar thermal conductivity. Also, the bipolar thermal conductivity has a sharp peak at $p = bn$ or $\sigma_{\mathrm{elec}} = \sigma_{\mathrm{hole}}$ in the intrinsic regime with varying carrier concentration at a given temperature, where $b = \mu_{\mathrm{elec}}/\mu_{\mathrm{hole}}$ is the mobility ratio between electrons and holes.

Fig. 1 shows the curve fitting results based on the electron transport modeling for the experimental data of the epitaxially grown p-type PbTe from Ref. 7 and the 2% Na-doped nanostructured PbTe from Ref. 9. We used the linearized Boltzmann transport equations under the relaxation time approximation for the calculations.[10] A multiple non-parabolic band model with temperature-dependent parameters was used to describe the band structure of PbTe.[7,22,23] Both the L-valley and the Σ-valley in the Brillouin zone were taken into account for the valence band. Recently, there

has been a controversy about the temperature-dependent band offset between the two valence bands of PbTe.[22,23] We chose 700 K as the band convergence temperature in this paper as suggested by Ref. 23. An online simulation tool for these Boltzmann transport calculations is available at nanoHUB.org.[24]

As shown in Fig. 1, the calculated Seebeck coefficients agree very well with the experimental values for both PbTe samples over the entire temperature range. In the calculations, a constant hole concentration of $5.2 \times 10^{18}\,\mathrm{cm}^{-3}$ was used for the epitaxial PbTe, whereas a temperature-dependent carrier concentration was used for the nanostructured PbTe, i.e., $1.2 \times 10^{20}\,\mathrm{cm}^{-3}$ at 300 K, which increases steadily with temperature to $1.9 \times 10^{20}\,\mathrm{cm}^{-3}$ at 900 K to account for the increased diffusion of Na dopant atoms into the matrix at higher temperature. The electrical conductivities of the epitaxial PbTe are very well fitted by the theory, but the calculated electrical conductivities of the nanostructured PbTe are higher than the experimental values, which imply that the carrier mobilities were reduced in the nanostructured material due to increased defect and grain boundary scatterings. The discrepancy between theory and experiment, however, becomes smaller as temperature increases, because the contribution of the additional scatterings becomes much weaker at higher temperature due to the increased phonon scattering. In Fig. 1, the calculated bipolar thermal conductivity is also compared with the extracted bipolar thermal conductivity by the linear extrapolation method described above for the nanostructured PbTe. The discrepancy between the calculated and extracted values can be largely due to the uncertainty in the linear extrapolation method. The bipolar thermal conductivity becomes as high as 0.28 W/m K at 900 K in the p-type PbTe with $1.9 \times 10^{20}\,\mathrm{cm}^{-3}$ hole concentration.

Alloying can increase the band gap and consequently reduce the bipolar thermal conductivity according to Eq. (2).[25,26] However, the increased band gap by alloying typically accompanies the increased valley effective masses of both types of carriers, which results in the reduction in the electrical conductivity and thus the power factor.[25] Instead, band engineering is often utilized to increase the valley degeneracy, i.e., via band convergence, to enhance the Seebeck coefficient.[16] However, it is not always easy to find a bulk semiconductor material with an appropriate band structure. This is the reason that heterostructures are employed to modify the transport of electrons or holes. Examples include type I and II superlattices used in semiconductor laser diodes or IR photodetector devices.[27] If a small direct bandgap semiconductor with appropriate electrical, optical, and mechanical properties existed, there would have been no reason to build complex quantum cascade lasers that emit in THz range.[28] Since an appropriate bulk material does not yet exist, researchers have used heterostructures in a large band gap material to get the appropriate electron transport and emission properties. In this paper, we show that a similar approach could be an important research direction in order to modify the bipolar thermal conductivity.

A significant suppression of bipolar transport is possible when the minority carriers are prevented from participating in conduction by incorporating heterostructure barriers in the
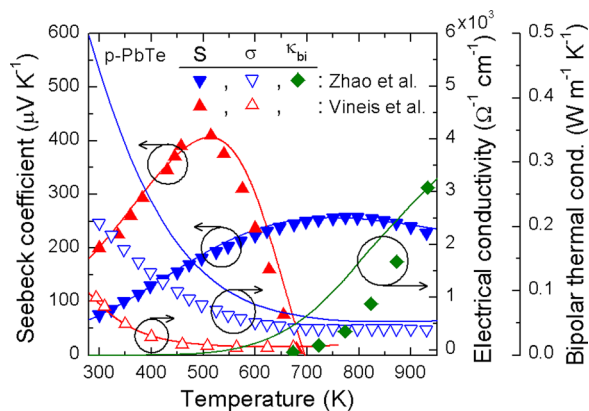

FIG. 1. Experimental Seebeck coefficients (left y-axis), electrical conductivities (first right y-axis), and bipolar thermal conductivities (second right y-axis) for the epitaxially grown p-type PbTe with $5.2 \times 10^{18}\,\mathrm{cm}^{-3}$ hole concentration from Ref. 7 and the 2% Na-doped nanostructured PbTe from Ref. 9 as a function of temperature and their corresponding fitting curves from our Boltzmann transport modeling. Symbols are the experimental data and solid curves are the fitting results.

target material. The barriers must be one-sided such that transport of majority carriers is not much affected by the heterostructures. This minority carrier blocking scheme is illustrated as a schematic band diagram in Fig. 2.[29] Transport of minority carriers, electrons in this case, is blocked by high barriers formed by the heterostructures that have a large conduction band offset but a negligibly small valence band offset between the well and barrier materials. One example of such a heterostructure could be p-type PbTe:SrTe system,[30] in which SrTe has a relatively large band offset with PbTe in the conduction band, while there is a negligibly small band offset in the valence band. It is desirable to have the barrier width large enough to prevent tunneling. The barriers can be either planar as in superlattices or nonplanar with nanoparticles dispersed in the bulk. Note that these barriers can also help reduce the lattice thermal conductivity via increased phonon scatterings at the boundaries or modification of phonon dispersion in the case of a periodic structure.[11]

In addition, it is important to address the requirement for the average inter-barrier spacing for successful realization of the minority carrier blocking scheme. If the inter-barrier spacing is too large, i.e., much larger than the electron mean free path, transport between two adjacent barriers is bulk-like. Bipolar transport with thermodiffusion phenomenon can occur similar to bulk in each of the segments between barriers. If the inter-barrier spacing is on the order of the electron mean free path, typically a few tens of nanometers, the bulk limit is broken, and minority carriers are trapped within the nanoscale region between the barriers. The bipolar thermodiffusion process that exchanges thermal energies with the lattice via regeneration/recombination of electron-hole pairs will not occur because there is no drive for extra carrier regeneration or recombination with local minority carriers largely confined, thus resulting in the suppression of bipolar thermal conduction.

Fig. 3 shows the calculated thermoelectric transport properties of p-type PbTe with minority carrier blocking as a function of carrier concentrations at 900 K. Here, we

assumed a significantly high barrier ($>10 k_B T$) in the conduction band to effectively block most of the minority carrier (electrons) transport even at low hole concentrations. A relatively small barrier height (50 meV) is assumed for the
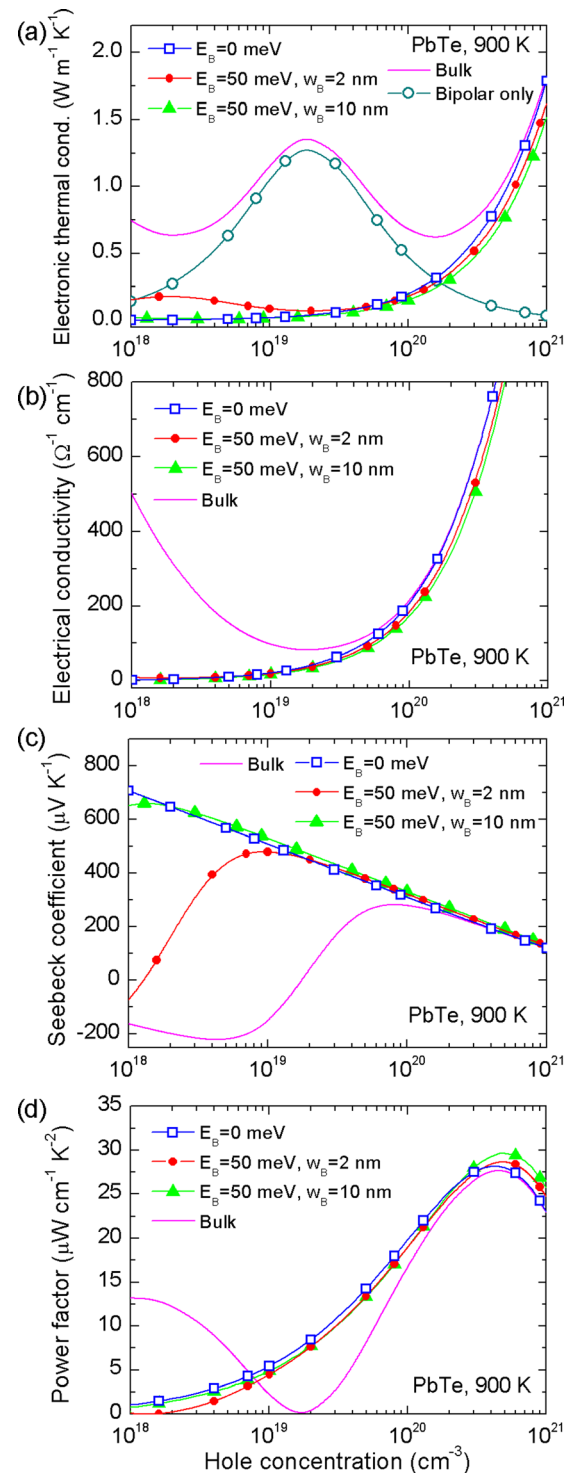
FIG. 3. Calculated (a) electronic thermal conductivity, (b) electrical conductivity, (c) Seebeck coefficient, and (d) power factor of p-type PbTe with minority carrier (electron) blocking as a function of hole concentration at 900 K. A very large barrier height ($=10 k_B T$) was assumed for electrons, and zero or a relatively small barrier height ($E_B = 0$ and 50 meV) were assumed for holes. Two barrier sizes ($w_B = 2$ and 10 nm) were considered and the modified transmission probability through the barriers was obtained using the WKB approximation. Bulk properties are plotted together for comparison.
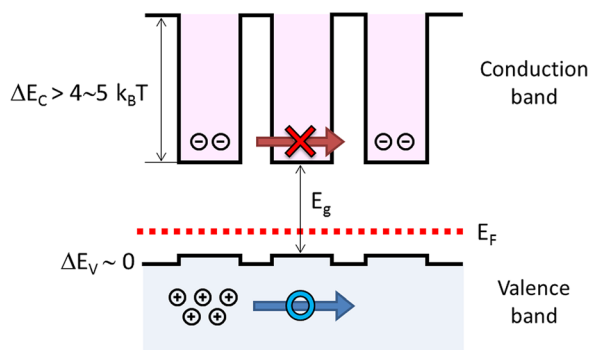
FIG. 2. Schematic band diagram of the proposed heterostructures for minority carrier blocking. Holes are majority carriers in this case. High barriers are formed by a large band offset (>4–5 $k_B T$) in the conduction band for electron blocking, whereas almost no band offset in the valence band for seamless conduction of majority holes through the hetero-interfaces. Average inter-barrier spacing is required to be on the order of the electron mean free path. Barriers can be either planar as superlattices or nonplanar as nanoparticles embedded in a bulk material. Similarly, barriers in the valence band can be used for n-type material. (see Ref. 29, where a similar band structure is proposed for power factor enhancement.)

majority carriers, and two barrier sizes, 2 and 10 nm, are considered. These barriers impose modified transmission probability in the differential conductivity calculation determined by the Wentzel-Kramers-Brillouin (WKB) approximation.[31] The use of transmission probability by the WKB approximation is valid when the barrier size is thinner than the electron energy relaxation length (10–30 nm) but larger than the electron de Broglie wavelength (a few nm). In this case, we are in a regime where the properties of the composites can be very different from each of the materials used in wells or barriers and also different from the "average" alloy of the two materials.

As shown in Fig. 3(a), when there is no minority blocking, the bipolar thermal conductivity has its maximum value ~ 1.3 W/m K at 2×10^{19} cm^{-3} hole concentration for PbTe at 900 K. Note that the hole and electron concentrations are mutually coupled with a single Fermi level in the band structure and are inversely proportional to each other at a given temperature. As either the hole or electron concentration increases to the right or left x-axis direction in Fig. 3(a), respectively, the bipolar thermal conductivity steadily decreases from the maximum point, since it is deviating from the intrinsic region, whereas the unipolar electron or hole thermal conductivities increase in proportion to their corresponding carrier concentrations. Thus, there is a minimum of the total bulk thermal conductivity ~ 0.6 W/m K for each majority carrier type. It is clearly shown in Fig. 3(a) that the electronic thermal conductivity can be significantly reduced in the intrinsic carrier region when the bipolar thermal conduction is suppressed. The 2 nm barrier width allows a small portion of minority carriers to transport via tunneling, so that there is non-negligible contribution from electrons in the electronic thermal conductivity as well as in the Seebeck coefficient at low hole concentration region.

The electrical conductivity is also reduced, since the contribution of the other carrier type is suppressed as shown in Fig. 3(b). The magnitude of the Seebeck coefficient is greatly enhanced when the bipolar contribution is suppressed; otherwise, the partial Seebeck coefficients of electrons and holes would cancel each other through bipolar transport as seen with the bulk curve in Fig. 3(c). As a result, the power factor is enhanced in the intrinsic region as shown in Fig. 3(d). However, near the optimal doping level for maximum power factor, the power factor enhancement is small because the corresponding optimal carrier concentration is quite far from the range of carrier concentrations where the Seebeck coefficient is significantly enhanced by the minority carrier blocking. It is also noted that at high hole concentration region, the power factor is slightly enhanced for the 50 meV barrier height in the majority carrier band due to the hot carrier energy filtering effect.[32]

We should point out some major differences between minority carrier blocking and the hot carrier energy filtering proposed to enhance the power factor.[12] In order to completely block the minority carrier transport, a very high barrier height is needed, whereas the energy filtering is to create a sharp contrast in the transmission between high-energy majority carriers and low-energy ones at a desired energy level. Thus, in the latter, the potential barrier must be very carefully designed, depending on the Fermi level position and

the temperature. Minority carrier blocking does not have strict requirements for appropriate barrier height or lateral momentum conservation.[12,32]

Fig. 4 presents the calculated figure of merit of PbTe with minority carrier blocking at 900 K. A constant lattice thermal conductivity of 0.3 W/m K was assumed for the calculations. As shown in the figure, the figure of merit can be greatly enhanced over the bulk maximum when the bipolar transport is suppressed by the minority carrier blocking for each type of carrier. For p-type PbTe, a maximum zT above 3.5 is possible at $1 \sim 2 \times 10^{20}$ cm^{-3} hole concentration with the minority carrier blocking (e-blocking) at 900 K when the lattice thermal conductivity is 0.3 W/m K. This is a more than 60% enhancement over the bulk maximum $zT \sim 2.3$ for p-type PbTe. The optimal hole concentration is lowered with the minority carrier blocking in order to take advantage of the large reduction of electronic thermal conductivity at lower electron concentrations near the intrinsic region.

For n-type PbTe, a similar approach can be taken with a large barrier in the valence band and a much smaller barrier in the conduction band for minority carrier blocking. A maximum zT above 2 is possible at 1–2×10^{19} cm^{-3} electron concentration (3–4×10^{18} cm^{-3} hole concentration) by the minority carrier blocking (h-blocking) at 900 K when the lattice thermal conductivity is 0.3 W/m K. This is an about 90% enhancement over the bulk maximum $zT \sim 1.2$ for n-type PbTe. If the lattice thermal conductivity is higher, the zT enhancement for both carrier types will be smaller because the bipolar contribution in the total thermal conductivity becomes relatively smaller. Still, a large $zT \sim 2.8$ is possible for p-type PbTe, and a $zT \sim 1.6$ for n-type PbTe by the minority carrier blocking when the lattice thermal conductivity is 0.5 W/m K according to the calculations.
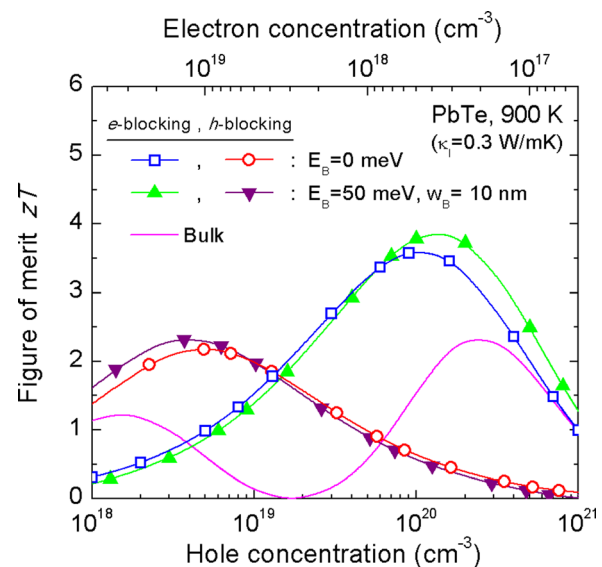

FIG. 4. Calculated thermoelectric figure-of-merit zT of PbTe with the minority carrier blocking for each carrier type at 900 K as a function of hole (bottom x-axis) and electron (top x-axis) concentrations. A very large barrier height ($=10k_BT$) was assumed for minority carriers, and a relatively small barrier height ($E_B = 0$ and 50 meV) of 10 nm size was assumed for majority carriers. A constant lattice thermal conductivity of 0.3 W/m K was assumed in the calculations. Bulk values are also shown for comparison.

In summary, our analysis in this paper highlights the importance of bipolar thermal conductivity reduction for the enhancement of thermoelectric figure of merit, particularly in small band gap materials at high temperatures. Careful electron transport modeling is required to accurately analyze experimental thermal conductivity data which include both lattice and electronic contributions. We propose the use of heterostructures, either planar or nonplanar, that create high barriers in the minority carrier band to suppress the detrimental bipolar effects. Usually, thermoelectric materials are highly doped in order to prevent bipolar transport. If the minority carrier blocking is realized, as proposed in this paper, a much lower carrier doping range can be utilized to achieve a very large figure of merit.

[1]L. E. Bell, Science **321**, 1457 (2008).
[2]K. Yazawa, Y. R. Koh, and A. Shakouri, Appl. Energy **109**, 1 (2013).
[3]J. A. Cape and G. W. Lehman, J. Appl. Phys. **34**, 1909 (1963).
[4]D. G. Cahill and R. O. Pohl, Phys. Rev. B **35**, 4067 (1987).
[5]C. A. Paddock and G. L. Easley, J. Appl. Phys. **60**, 285 (1986).
[6]C. L. Tien, A. Majumdar, and F. M. Gerner, *Microscale Energy Transport* (Taylor & Francis, Washington, DC, 1998).
[7]C J. Vineis, T. C. Harman, S. D. Calawa, M. P. Walsh, R. E. Reeder, R. Singh, and A. Shakouri, Phys. Rev. B **77**, 235202 (2008).
[8]H. Wang, J.-H. Bahk, C. Kang, J. Hwang, K. Kim, A. Shakouri, and W. Kim, J. Mater. Chem. A **1**, 11269 (2013).
[9]L. D. Zhao, H. J. Wu, S. Q. Hao, C. I. Wu, X. Y. Zhou, K. Biswas, J. Q. He, T. P. Hogan, C. Uher, C. Wolverton, V. P. Dravid, and M. G. Kanatzidis, Energy Environ. Sci. **6**, 3346 (2013).
[10]J.-H. Bahk and A. Shakouri, in *Nanoscale Thermoelectrics*, Lecture Notes in Nanoscale Science and Technology, Vol. 16, edited by X. Wang and Z. Wang (Springer, Switzerland, 2014), Chap. 2, pp. 41–92.
[11]C. J. Vineis, A. Shakouri, A. Majumdar, and M. G. Kanatzidis, Adv. Mater. **22**, 3970 (2010).
[12]A. Shakouri, Annu. Rev. Mater. Res. **41**, 399 (2011).
[13]M. Zebarjadi, K. Esfarjani, M. S. Dresselhaus, Z. F. Ren, and G. Chen, Energy Environ. Sci. **5**, 5147 (2012).
[14]K. Biswas, J. He, I. D. Blum, C.-I. Wu, T. P. Hogan, D. N. Seidman, V. P. Dravid, and M. G. Kanatzidis, Nature **489**, 414 (2012).
[15]Y. Pei, A. LaLonde, S. Iwanaga, and G. J. Snyder, Energy Environ. Sci. **4**, 2085 (2011).
[16]Y. Pei, X. Shi, A. LaLonde, H. Wang, L. Chen, and G. J. Snyder, Nature **473**, 66 (2011).
[17]Y. Pei, N. A. Heinz, A. LaLonde, and G. J. Snyder, Energy Environ. Sci. **4**, 3640 (2011).
[18]K. Ahn, K. Biswas, J. He, I. Chung, V. David, and M. G. Kanatzidis, Energy Environ. Sci. **6**, 1529 (2013).
[19]W. Liu, X. J. Tan, K. Yin, H. J. Liu, X. F. Tang, J. Shi, Q. J. Zhang, and C. Uher, Phys. Rev. Lett. **108**, 166601 (2012).
[20]J.-H. Bahk, Z. Bian, and A. Shakouri, Phys. Rev. B **89**, 075204 (2014).
[21]J. R. Drabble and H. J. Goldsmid, *Thermal Conduction in Semiconductors* (Pergamon Press, New York, 1961).
[22]C. M. Jaworski, M. Nielsen, H. Wang, S. Girard, W. Cai, W. Porter, M. G. Kanatzidis, and J. P. Heremans, Phys. Rev. B **87**, 045203 (2013).
[23]Z. Gibbs, H. Kim, H. Wang, R. L. White, F. Drymiotis, M. Kaviany, and G. J. Snyder, Appl. Phys. Lett. **103**, 262109 (2013).
[24]J.-H. Bahk, R. B. Post, K. Margatan, Z. Bian, and A. Shakouri, "Linearized Boltzmann transport calculator for thermoelectric materials," https://nanohub.org/resources/btesolver.
[25]Y. Pei, H. Wang, and G. J. Snyder, Adv. Mater. **24**, 6125 (2012).
[26]J. Yang, S. Wang, J. Yang, W. Zhang, and L. Chen, MRS Proc. **1490**, 9–18 (2013).
[27]L. A. Coldren, S. W. Corzine, and M. L. Mašanović, *Diode Lasers and Photonic Integrated Circuits*, 2nd ed. (Wiley & Sons, New Jersey, 2012).
[28]B. S. Williams, Nat. Photonics **1**, 517 (2007).
[29]P. G. Burke and J. E. Bowers, "Incorporating minority charge carrier blocking regions with thermoelectric materials for improved thermoelectric device efficiency," University of California Invention Disclosure, filed on 20 November 2013.
[30]L. D. Zhao, V. P. Dravid, and M. G. Kanatzidis, Energy Environ. Sci. **7**, 251 (2014).
[31]D. J. Griffiths, *Introduction to Quantum Mechanics* (Prentice-Hall, London, 1995).
[32]J.-H. Bahk, Z. Bian, and A. Shakouri, Phys. Rev. B **87**, 075204 (2013).